MEASURING 3D COASTAL CHANGE WITH A DIGITAL CAMERA

Mike R. James[1], Suzana Ilic[2], Igor Ruzic[3]

Abstract

We explore the use of digital photography for reconstructing topographic data of coastal regions using 'structure from motion' (SfM) algorithms. 3D models are constructed from photographs taken from different positions in a workflow that offers significant simplifications in terms of data acquisition and automated processing, over traditional photogrammetry. Two different SfM implementations (one based on a local PC and the other on a web-based service) are demonstrated for quantifying surface change over different spatial scales - a subaerial beach, a cliff face and scour holes around vegetation tussocks. The results indicate that SfM is a promising tool for morphological measurement, capable of cheaply producing data that can be of a comparable accuracy to other commonly used techniques.

Key words: Remote-sensing, digital camera, structure-from-motion, digital elevation models, coastal change.

1. Introduction

Various remote sensing techniques have been made available to coastal scientists and managers in the last decade or so. Techniques such as airborne Light Detection and Ranging (LIDAR e.g. Stockdon et al. 2002) and space-based radar and video imaging (e.g. ARGUS system, Plant and Holman, 1997) as well as photogrammetric techniques are used to derive digital elevation models (DEMs) which have been used to enhance our understanding of coastal changes at different spatial and temporal scales. All of these have advantages and limitations in terms of spatial and temporal coverage, expertise and software needs, and costs. For example over spatial scales of 10's – 100's of meters, ground-based terrestrial laser scanners (TLS) are being increasingly used (e.g. Rosser et al., 2005). While their accuracy and ranges are increasing, and weight and cost decreasing, they still require significant expertise in data acquisition and processing. Airborne LIDAR allows the rapid collection of data over larger areas (km scales) at high spatial density. Elevations derived from these data have a vertical accuracy of order of 1 decimetre, which is smaller than beach changes caused by large storms (Sallenger et al., 2003). Hence, such data may be used for detailed spatial analysis of variability of coastal areas. However, LIDAR surveys may only be made infrequently due to high cost and the careful organisation required, leading to a sparse temporal coverage. In contrast, video imaging systems such as ARGUS permit studies of high temporal variability (Harley et al. 2011). Images are collected over areas of 100m to several km, with temporal intervals ranging from 10min – 1h. Such imagery has been successfully used to derive shoreline locations and 3D topography of intertidal beaches for little cost. However, all of these methods need specialist analysis software, which might not be available to all coastal managers.

An alternative and complementary approach is presented here, based on freely available 'structure-from-motion' (SfM) computer vision software or web service that creates 3D models from field photographs taken by a single consumer-grade camera. The algorithms are designed to work with convergent imagery and require a number of photos to be taken from different locations. However, unlike traditional photogrammetry, for initial model reconstruction, the algorithms do not need any additional camera information or field control points, and involve little or no operator intervention. The camera used can be

[1] Lancaster Environment Centre, Lancaster University, Farrer Avenue, Lancaster, LA1 4YQ, UK. m.james@lancaster.ac.uk
[2] Lancaster Environment Centre, Lancaster University, Farrer Avenue, Lancaster, LA1 4YQ, UK. s.ilic@lancaster.ac.uk
[3] Faculty of Civil Engineering, University of Rijeka, R, Matejčić, 3, 51000 Rijeka, Croatia. igor.ruzic@gradri.hr

easily mounted on different platforms such as on light weight unmanned aerial vehicles (UAVs).

Two SfM implementations have been used here; firstly, a freely available 'reconstruction pipeline' (see James and Robson (2012) for details) that runs locally on a PC and combines the SfM application 'Bundler' (Snavely et al. 2008) with a 'multiview stereo' (MVS) dense image matcher 'PMVS2' (Furukawa and Ponce, 2010), and secondly, the free web service 123D Catch, developed by Autodesk® (http://www.123dapp.com/catch). Both are free to use and require multiple images of a scene taken from different positions. This paper illustrates application of this approach for assessing erosion of a coastal cliff, variability around a vegetation tussock on an intertidal flat, and change over a pocket gravel beach.

2. Methodology

All field photographs were taken with a hand held digital SLR camera (Canon EOS 450D) and fixed focal length lenses. James and Robson (2012) gave several recommendations for collection of images in order to produce accurate 3D reconstruction. Wide angle lenses (e.g. equivalent to 35mm on traditional SLR cameras) should be used. Shots should be taken over wide range of angles with intervals of 10-20^{o} allowing the camera orientation to converge on the area of interest. The procedure allows collection of more images than necessary to reduce the chance of accidentally omitting some of the areas. Ideally the illumination conditions should be diffuse to avoid strong shadows and should not contain reflections. For good image sets, relative reconstruction precisions (3D point coordinate precision: mean camera viewing distance) are expected to be ~1:1000 (James and Robson, 2012).While the methods can handle the images taken at different scales, photos taken by using large zooms or at significantly different distances to the surfaces of interest can cause the images to be omitted from the final model.

The collected images are then processed with the freely available software. Of order 10-100 photographs are uploaded to a PC for 3D reconstruction when using the SfM-MVS method described by James and Robson (2012). For using 123d Catch, photographs are uploaded to the Autodesk cloud. The methods work by matching image texture in different photographs, and determining the 3D geometry under the assumption that the scene is static. The SfM process initially detects prominent features in the images and matches them between different images. This matching is then used to derive camera model parameters, camera orientations and to compute 3D coordinates for the feature points (the sparse point cloud). A dense matcher (e.g. PMVS2) is then used to derive detailed point clouds. Surfaces without prominent texture (e.g. flat sandy beach or areas in strong shadow) as well as those with overlapping vegetation stems and moving leaves (Castillo et al., 2012) will not be reconstructed.

The reconstructed 3D models have arbitrary scale and require geo-referencing. For locally run SfM-MVS reconstructions, the sfm_georef tool of James and Robson (2012) was used to geo-reference models from control points identified in the images. For web-processed models from 123D Catch, Matlab® scripts were developed to enable geo-referencing from control point identification in the surface data. Required transformations (scaling, rotation and translation) are derived by matching 3D coordinates derived by the reconstruction software with the coordinates of identified control points. The control points should be located toward the edge or just outside the area of interest. A minimum of three control points are required but more give more robust solutions and allow for better error estimation. For absolute referencing, the coordinates of control points can be obtained using a RTK-GPS or a total station as in other remote sensing techniques. Details of the procedure used in each of the application presented here are given below.

3. Applications

3.1. *Assessing erosion of a coastal cliff*

Erosion of soft coastal cliffs has been a subject of numerous studies (e.g. Greenwood and Orford, 2008, Young et al., 2009). Most of them are of glacial origin and consist of rocks that have little resistance, such as clays, shales or sandstone or unconsolidated material such as sand. Due to this, they are susceptible to erosion, which can occur either through sudden slope failures or through gradual removal of sediment from

the cliff face, as a result of both marine and subaerial erosion mechanisms. Traditionally, changes on cliff faces were measured by using erosion pins. Whist providing important information of cliff retreat, the sparse spatial coverage did not allow the assessment of spatial variability in erosion rates and volumes. The alternative methods such as airborne and ground-based LIDAR, as well as photogrammetry, provide much better spatial coverage, which enabled detailed geostatistical and geotechnical analysis of cliff changes (for more details see James and Robson, 2012). Therefore any alternative method should provide similar or better spatial coverage with at least similar accuracy, and should reduce the time required for data acquisition and generation of DEMs or surface models. The SfM-MVS method has the potential to achieve this.

The cliff at Sunderland Point is composed of unconsolidated, poorly sorted glacial tills and is undergoing retreat through intermittent slumping and collapse. It is situated at the mouth of the Lune estuary in a macro-tidal environment with a mean spring tidal range of 10.5m (-4.5 to +6.0 O.D.) and mean neap tide range of 3.4m (-1.4 to +2.0m O.D.) (French and Livesey, 2000). The dominant wind directions are from the west and south west (Moxon, 2011). The wind generated waves are of limited fetch, greatest being of approximately 225 km and located to the south west of Sunderland Point. At spring tides, the waves can reach the base of the cliff.

The locally run SfM-MVS algorithms were successfully used to assess erosion of a ~3-m-high and 50-m-long section of coastal cliff located at Sunderland Point, Morecambe Bay, UK, between February 2011 and March 2012 (James & Robson, 2012). The quality of the SfM-MVS reconstructions was assessed by a comparison with a simultaneously acquired terrestrial LIDAR survey (TLS). Differences were <20mm over much of the cliff face (James and Robson, 2012) and were comparable to the accuracy of the TLS instrument. The same procedure has been applied for surveys taken between March and December 2012 reported here.

Figure 1. The images taken at Sunderland points on 18th August, 13th October and 28th December 2012.

Series of photographs (excerpts of which are shown in Figure 1) were taken at ~2m intervals on five occasions between March and December 2012, covering a collapse event and erosion of the cliff foot. As in previous work, a Canon EOS 450D camera with a 28mm fixed focal length lens was used for image acquisition and ~100-130 photographs were used for each 3D reconstruction. Eight control points (the tops of groyne and fence posts, with coordinates known from GPS and TLS data) were used to scale and geo-reference the SfM-MVS reconstructions, with residual errors of ~50 mm or less. To enable a fuller comparison of data across the cliff face, the point clouds have been converted to raster-based surfaces by gridding them within a vertically-oriented cylindrical coordinate system as shown in Figure 2.

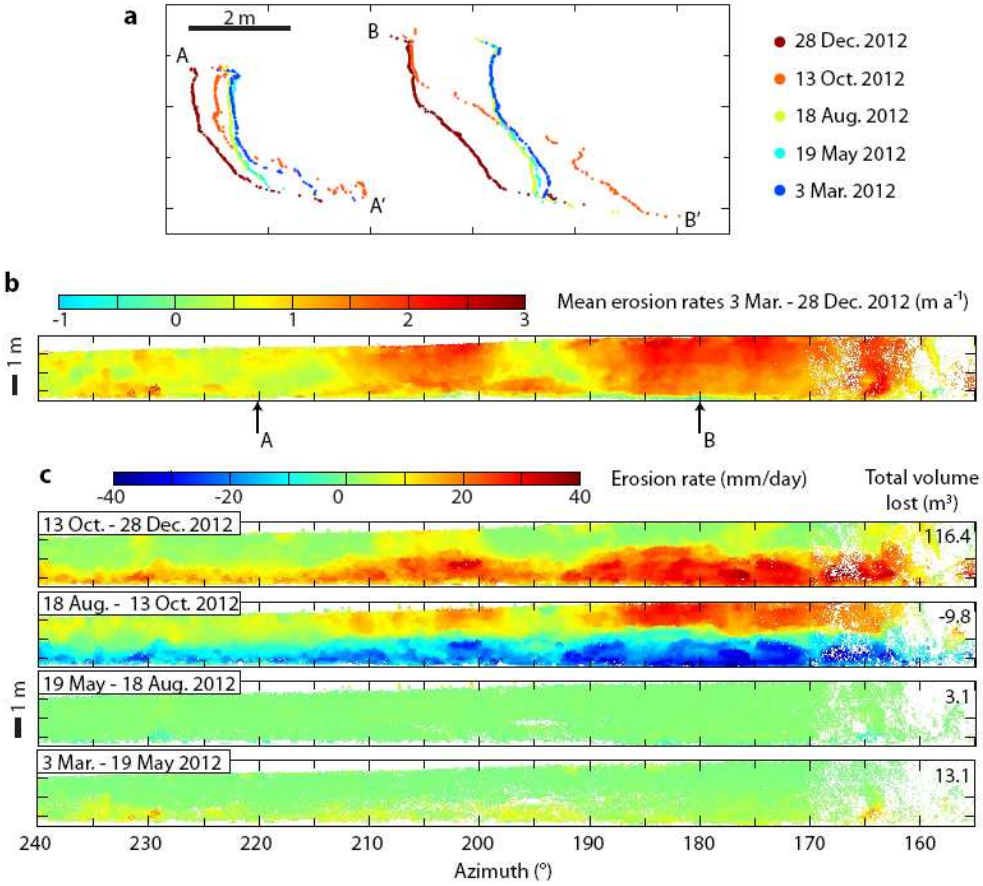

Figure 2. Erosion rates at Sunderland Point. a) Cross-sections through the raw SfM-MVS data for the surveys taken at five occasions. b) Change between the first and last surveys, expressed as an erosion rate map (negative values indicate deposition – seaward movement) derived by differencing the cylindrical gridded models (azimuth values represent approximately 0.05m per degree). The arrows indicate the locations of the profiles given in a). c) Sequential erosion maps calculated between surveys on the given dates.

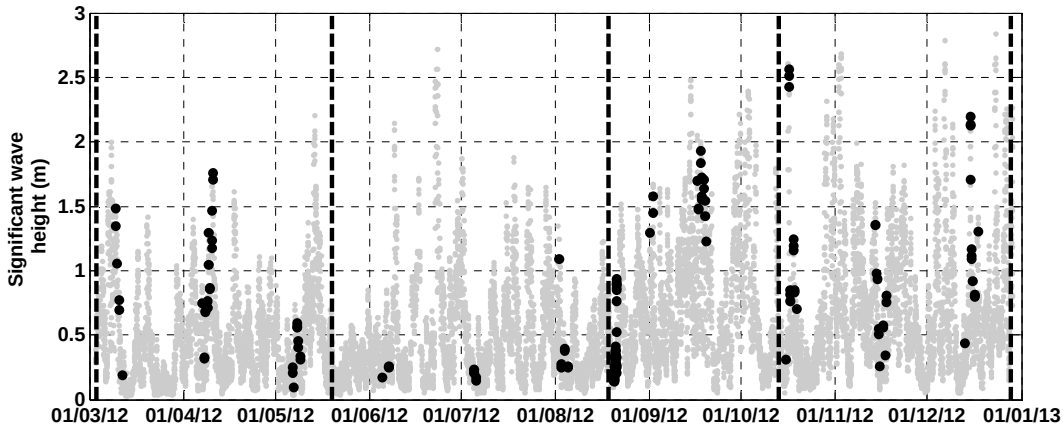

Figure 3. Significant wave height measured at Morecambe Bay buoy from 3rd March – 28th December 2012. The bold points show the events with the wave directions between 203-293 ^{o} (SSW and WNW) measured at water level above +5.0 OD.

Figure 2 shows the changes and erosion rates derived from images taken on five occasions. Figure 2b shows that mean erosion rates of 1-3m per year over the whole cliff face. However, erosion was not evenly distributed. The southern cliff face, close to the estuary (between 155-200^{o}), experienced the maximum erosion, following by the area between 200-210^{o} on the opposite side of the tip of the cliff. The temporal variability has been clearly shown in Figures 2c and 2a. Between two first surveys, material has been moved mostly from the cliff base, more at the northern than southern foot (Figure 2a). There have been hardly any changes observed between second and third survey. Between third and fourth survey there has been a large collapse at the upper cliff face, in particular at the southern side close to the estuary. Most of the material remained deposited at the toe of the cliff at southern side but at northern side of the cliff material was completely removed. Between the surveys taken in October and December, the northern face retreated further inland while the changes that occurred at the southern side were mostly due to a removal of deposited material from the toe of the cliff.

A number of studies of cliff erosion (e.g. Greenwood and Orford, 2008) around the Irish Sea found that direct wave attack is an important factor in controlling cliff erosion. This is particularly valid during high tidal levels supported by storm surges created in the Irish Sea. Figure 3 shows the significant wave height recorded at the Morecambe buoy about 12km SW and offshore of Sunderland Point. The waves arriving from 203 and 293 ^{o} (SSW and WNW) during high tidal levels above +5.0 OD measured at Heysham (~4 km north of the site) were selected. During these conditions, the waves can reach the cliff toe of +5.4OD. A clear seasonality in the wave energy can be observed. Wave heights above 1.5m were recorded several times during spring months (March – May). This followed by a very low activity in summer months (May – August). Wave heights close to storm thresholds (2m) were recorded in mid September and in late autumn (October – December). This matches well with observed cliff erosion, highest being in periods with greatest measured wave energy. The debris deposited in the front of the cliff is most likely removed by marine processes as reported in previous studies (Moxon, 2011). The mechanisms behind a collapse of upper cliff face are more uncertain. Young et al. (2009) found that rainfall was responsible for triggering most of the observed cliff failures in their study of cliffs in Southern California but that marine mechanisms acted to accelerate cliff erosion. In contrary, Greenwood and Orford (2008) argued that while the rainfall increased erodability of the cliff material, it is not a frequent trigger for cliff failure.

There are several possible mechanisms behind the observed collapse. High water content in the cliff itself can reduce its compressive strength. The can be caused by excessive rainfall, by water rising from the submerged part at high tides or by a combination of both. Once the cliff losses its strength will be more prone to the effects of wave action either wave breaking or swash run-up. As the surveys were taken during favourable conditions (low tide and calm conditions) there is a lack of data on the exact timing of the failure and it remains unknown whether the collapse happened due to subaerial or marine processes or perhaps due to a combination of both. Nevertheless, the detailed models of cliff face derived from surveys show spatial and temporal variability of erosion and accretion and are useful for coastal managers. With careful planning of surveys (e.g. after storm events) they can be useful in identifying the driving mechanism behind the cliff erosion.

3.2. *Scour around a Spartina Anglica tussock*

Intertidal vegetation such as saltmarsh vegetation alters hydrodynamic forces from waves and currents and consequently has an effect on intertidal sediment dynamics. Detailed studies of depositional and erosional patterns that emerge around patches of intertidal vegetation as result of changes that take place in boundary layer around, over and inside those patches have been rare (Bouma et al. 2007). It is very difficult to measure these small changes around vegetation. One of the reasons is that these areas are not easily accessible. Also they require more elaborate field measurements as the changes in topography are very small. Traditionally, recording of distances between sticks, which were employed close to vegetation for a certain length of time, and ground level were made. To increase spatial coverage, boards are used sometimes. They are put on the top of the sticks and more measurements at regular intervals between sticks were made (e.g. Bouma et al. 2007). However, such measurements can take long time and limit how many vegetation patches can be covered during low tide. Hence there is a scope to develop a remote sensing

technique, which will enable easier collection of dense spatial data.

The measurements were taken around *Spartina Anglica* tussocks in a saltmarsh on an intertidal flat at Morecambe, Morecambe Bay, UK. The saltmarsh is located in the north-easterly part of a groyne field between the West End and Battery groynes. Since groyne construction in 1992, significant sedimentation, primarily of fine silts and clays took place (French and Livesey, 2000), which led to the saltmarsh development. At spring tide, the tide covers the whole saltmarsh in about 45min, which stays submerged for more than an hour. At neap tide, the saltmarsh is uncovered except for *Spartina* tussocks on the lower mudlflats, which are partly covered with the water.

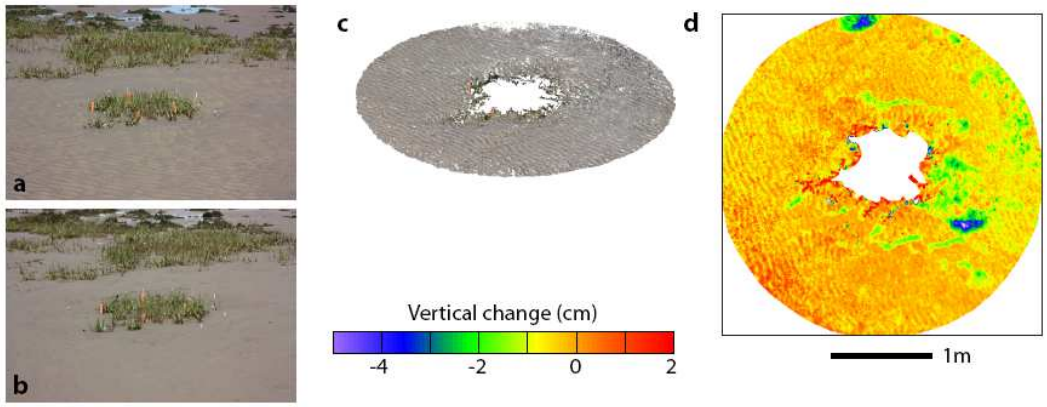

Figure 4. Digital elevation model of erosion and deposition around a Spartine tussock: a) photo taken on 20th June 2011; b) photo taken on 22nd June 2011; c) point cloud created for the image taken on 20th June 2011; d) difference map between 22nd and 20th June 2011.

Images were taken daily through a spring-neap tidal cycle in June-July 2011, to cover an area of a few m^2 around two tussocks. Photos were shot in 360^o loops and from different vertical heights. A Canon EOS 450D camera with 50mm fixed lens was used. The same procedure as for a study of the cliff erosion was applied for processing of the images and transforming them into the digital elevation models. Here an array of sticks shown in Figure 4a and b was used for scaling and relative registration of the different digital elevation models. Measurements of topographic change were taken next to the sticks at the same time as photographs on most of days. Figure 4 shows the differences between surveys taken two days apart, with observed changes in range of -4 to 2cm. Depositional areas close to the vegetation tussock and few erosional patches further away from the tussock can be clearly seen. However, most of changes are associated with bed ripple migration, indicating that the method can detect small changes in order of few centimetres very well. It was not possible to make the direct comparison of changes derived from images with those measured around fixed sticks but they seem to be of the same order of magnitude. The surfaces where the vegetation is present, inside the tussock and immediate vicinity of the tussocks, were not reconstructed. However, the method provided more detail around tussocks and was quicker to implement than traditional field measurements of scour.

3.3. *Volume changes of a pocket beach*

Most beaches on the Croatian coast are small pocket gravel beaches (with lengths from 50 m to couple of km) formed by the deposition of sediment from torrential flows. These beaches are affected by both natural and man-made changes in the catchment. As they are important not only for natural coastal protection but also for beach tourism and hence for the economy of the country, a sustainable protection scheme needs to be developed. This requires understanding of the natural dynamics of the sediment sources, sinks and sediment transport under different environmental conditions. Most beaches are situated in coves,

surrounded by steep headlands and slopes with limited accessibility. Hence, remote sensing techniques that do not require carrying heavy equipment are desirable.

123D Catch was used to assess the changes in morphology of a pocket gravel beach at Uboka cove (Figure 5a) located at the western edge of Kvarner Bay in the Northern Adriatic, Croatia. This beach, which is 70m long and 10-18m wide, remains relatively unmodified by human intervention and provides an ideal site for studies of the important natural processes that drive beach dynamics. The beach is micro-tidal with a mean spring tidal range of 1.62m (-0.57 to +1.05m vertical datum of the Republic of Croatia (VD)) and mean neap tidal range of 0.82m (-0.17 to +0.65m VD). It is exposed to wind waves from the South West and North East during winter and from South during the spring and summer months. The sediment (average grain size ~3cm) is derived from carboniferous rocks in the catchment of the Uboka torrential stream. The catchment is characterised by a karst geomorphology, having steep slopes of almost 1:1, high permeability and groundwater springs. The average annual rainfall is between 1500 and 2000mm, of which the majority falls during the autumn and winter. Rainfall intensities are high causing torrential flows and groundwater springs around the torrential channel to become active during the autumn and winter, but only occasionally during the spring and summer. The torrential flow breaches the beach and moves the sediment nearshore where is deposited in a lobe. The sediment is then returned back to the beach by coastal processes when the flow reduces.

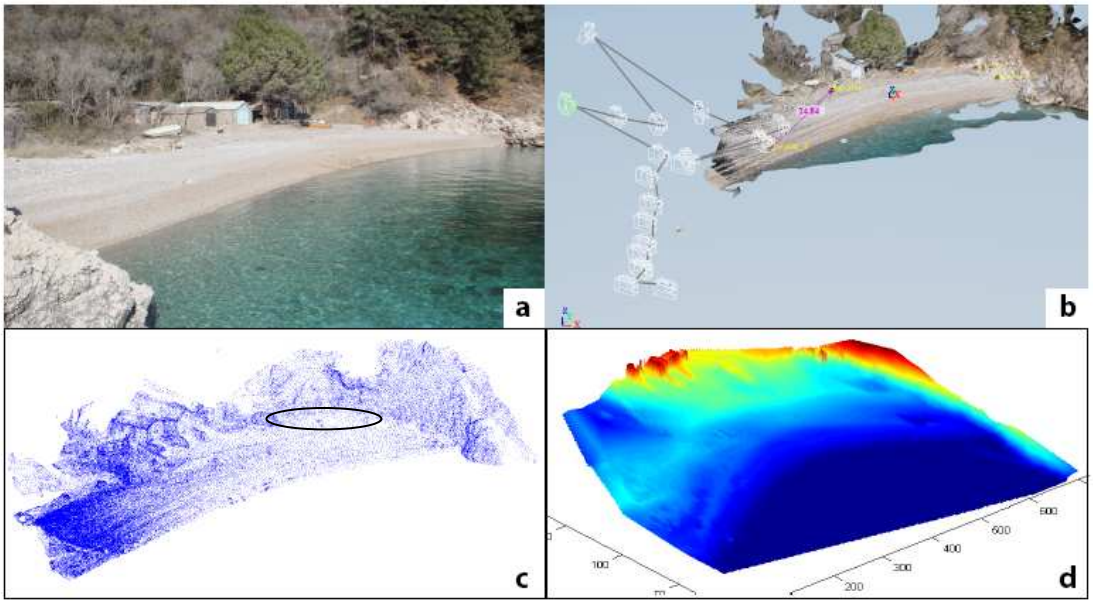

Figure 5. Reconstruction of a beach digital elevation model at Uboka cove: a) photo taken from one of the locations close to the beach; b) locations from which photos were taken; c) a point cloud derived by 123d Catch, the area which is 'static' is shown with black circle; d) digital elevation model obtained using a point cloud and geo-referencing transformation tools written in Matlab®.

A series of surveys, using a Canon EOS 450D camera with a 28mm fixed focal length lens, were carried out between January and May 2012 at low tide and during calm weather conditions. The local terrain configuration enabled taking photos of the whole beach from a range of different horizontal and vertical angles (Figure 5b). From photographs acquired in the field, 6-40 photos were chosen each time and uploaded to 123d Catch. In order to scale and geo-reference the 123d Catch reconstructions (Figure 5c), a Matlab® tool was written to identify the coordinates of 9 distinct points which were expected to be consistent through all surveys. The control coordinates for these points were obtained from dGPS surveys. The point clouds (Figure 5c) have been converted to raster-based surfaces and transformed into Gauss-Krüger coordinate system. Model errors were estimated by calculating differences in vertical elevation of an area believed to be static. This area is located in the furthest away corner from the camera track (Figure

5b) and also has the poorest cloud point density (Figure 5c). Calculated vertical error was ~5 cm, which is up to twenty times smaller than the largest detected changes.

From the 3D beach face reconstructions, the common area covered by all surveys was identified (Figure 5d). These were then used to derive several morphometric parameters. Here we consider the beach volume changes and changes in beach profiles. The surveys started immediately after a decrease in the torrential flow and covered the subsequent beach changes during several calm and stormy periods. Figure 6 shows the wind speed and direction measured at Mošćenička Draga weather station (DAVIS), ~3km to the NE. Between two first surveys (05/01-24/01/2012) wind speeds are below 5m/s and the dominant wind direction is from the west. Between second and third (24/01-05/02/2012) and third and fourth (05/02-17/02/12) surveys, the wind direction changed to predominantly north-easterly and averaged speed increased up to 8-9m/s and 13-14m/s respectively. During the period before the last survey (11/04/2012), the wind was blowing from the west and the north-east but for the most of the time wind speeds were below 5m/s. Hence the most wave activity in Uboka cove was between second and third and third and fourth survey.

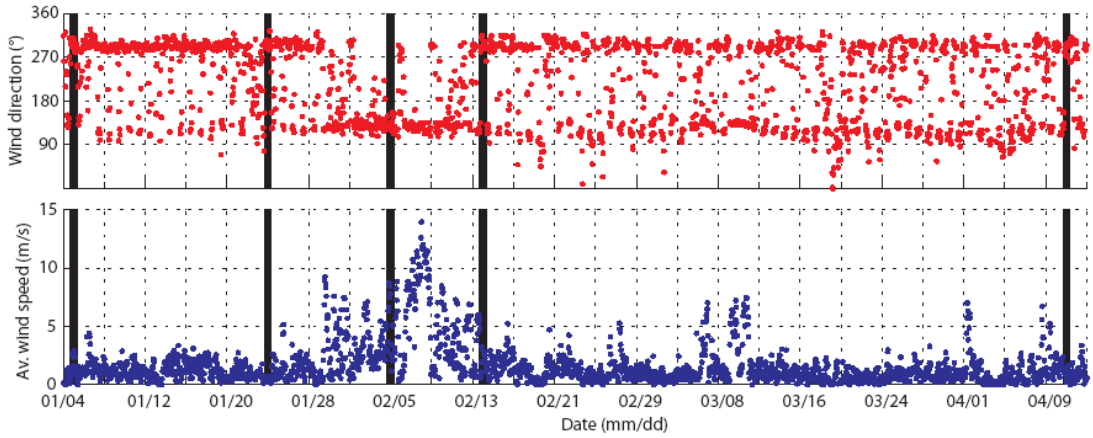

Figure 6: Wind conditions between 4th January and 13th April 2012 at the meteorological station Mošćenička Draga, close to Uboka cove; vertical lines show times when beach surveys were taken.

Figure 7 shows the beach changes between surveys. Overall there is accretion at the upper beach face between profiles 5 and 6 and, to some level, at the lower beach face between profiles 1 and 2, while erosion is observed between profiles 3 and 4 (Figure 7a). Most of changes occurred between surveys 1 and 2 and, in particular, between surveys 2 and 3. Despite being a relatively calm period between 5th and 24th January, the sediment from the lobe was transported onshore into the torrential channel once the torrential flow reduced. Potentially, this could have happened only few days before the survey when the wind was blowing from the south-west direction. Between 24th January and 5th February, the beach was exposed to waves driven by north-easterly wind which were partly refracted and partly broken at the lobe. The nearshore waves and currents transported material onshore from the lobe into the torrential channel and longshore from the central area between profiles 3 and 4 to the left and right sides of the beach. The beach changes were much smaller and evenly distributed during the second stormy period (between 5th and 17th February) and minimal between 17th February and 11th April.

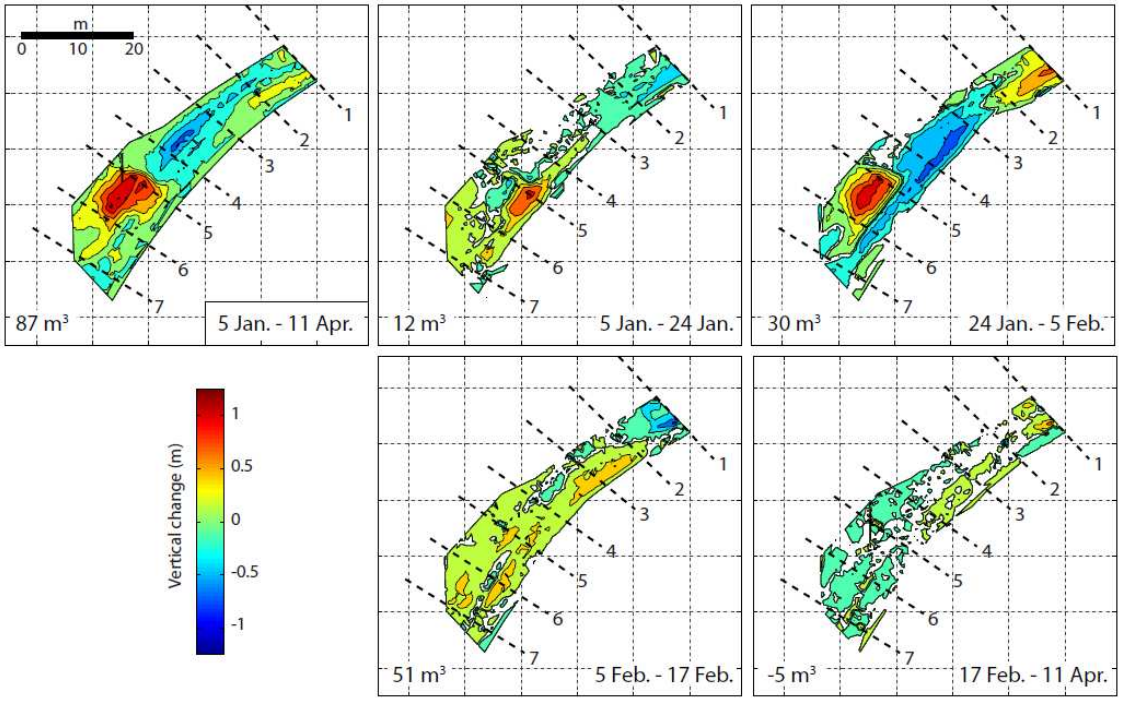

Figure 7: Changes in beach elevations between: a) first and last survey (05/01-11/04/2012); b) first and second survey (05/01-24/01/2012); c) second and third survey (24/01-05/02/2012); d) third and fourth survey (05/02-17/02/2012); e) between fourth and last survey (17/02-11/04/2012).

Figure 8 shows changes in beach profiles at three different locations between surveys. Profile 2 has changed the least. The berm at the top of the beach face (around 2m above sea level) has been flattened by 17th February and a new one was formed lower down the beach (around 1m above sea level). There have been only small erosional and accretional changes at the lower beach face. Profile 5 in the torrential channel has changed the most. The new barrier at the seaward side of the channel was formed between 5th and 24th January, which expanded through the whole channel by 5th February. There has been slight accretion at the seaward side and the top of the barrier by 17th February. Profile 6 shows similar pattern as profile 5. The channel behind the berm seen on surveys taken in January has been filled in by 5th February. Only slight seaward and upward accreation has been observed from surveys taken on 17th February and 11th April. The berm has been formed at its initial level of 1m. During the high wave conditions, swash berm was formed on the top of the beach in Profile 2 and overwash occurred on Profiles 5 and 6 transporting sediment onshore and creating new high beach berm (1.25m above sea level). Just before survey of 17th February, the wind reduced its speed and direction, which resulted in formation of a berm at about 1-1.25m above water level along the whole beach.

The beach volumes for all DEMs were calculated from 0.3m level. All changes which were in range between -5 and +5cm, in accordance with estimated elevation error, were not taken into account. Overall, the beach volume increased by 87m^3, which is due to onshore transport of sediment from the lobe formed by deposition of washed out sediment by the torrential flow prior to the surveys. Some sediment was likely transported outside the area of interest during the first storm. During the second storm, most of the material was transported onshore. Similarly to field observations by Weir et al. (2006), the closure of the beach opening was achieved mostly through cross-shore sediment transport.

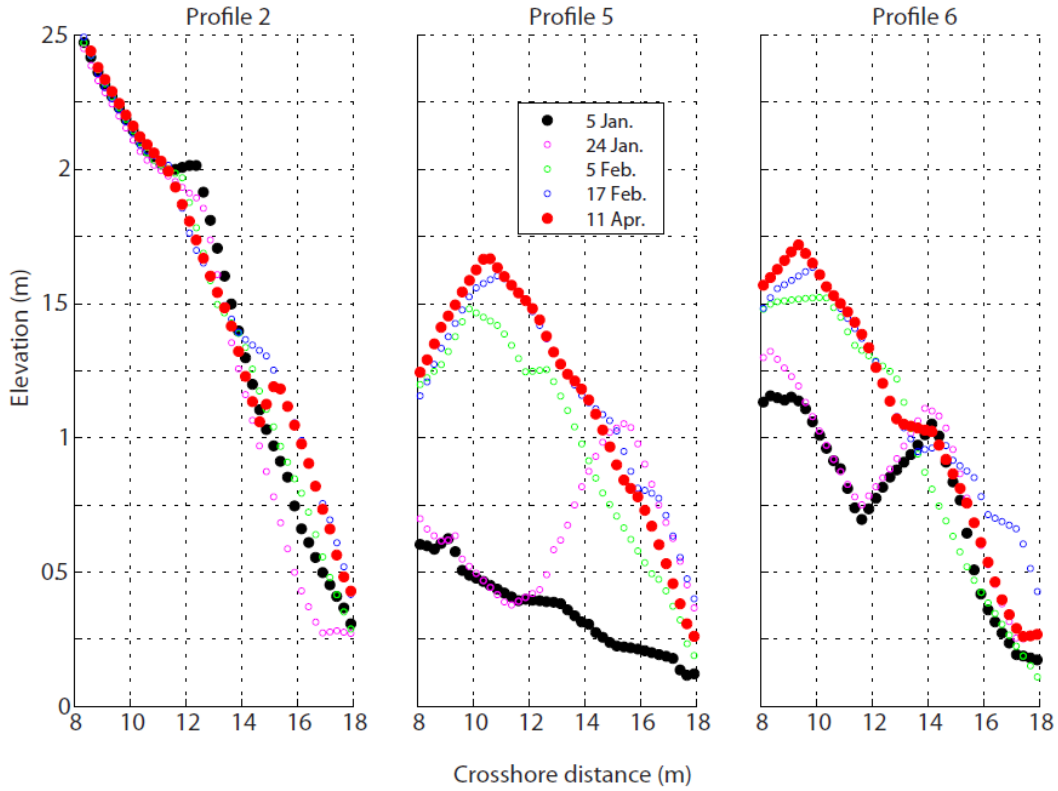

Figure 8: Beach profiles derived from digital elevations model at locations 2, 5 and 6 as given in Figure 6.

The pocket gravel beach is influenced by longshore and cross-shore sediment transport in the narrow surf and swash zone. The resulting beach changes are taking place over short time scales and have a distinctively 3D character. The digital camera surveys have been useful for identifying sediment transport patterns and general understanding of the beach face dynamics. The natural characteristics (e.g. sufficiently coarse material to give good image texture) and accessibility of these beaches make them ideal environments for 3D surveys using digital cameras.

4. Discussion

Despite the number of different approaches available for regular coastal monitoring and studies of coastal change, there is no single technique (Harley et al., 2011) capable of providing data over scales and scenarios relevant to a broad range of coastal applications. The case studies presented here (reconstruction of a subaerial beach, scour holes around vegetation tussocks and vertical cliff faces) demonstrate that SfM-MVS can be used to derive surfaces and topographies over wide spatial and temporal scales. The data can be collected remotely and by only one person at relatively low cost. There is minimal training needed before one can start with data acquisition and processing. The equipment is light and easy transportable to remote places and locations with low accessibility. These methods reduce time for field surveys, permitting more surveys for the same effort and offering significant opportunity for adoption by coastal managers. For example in case of the cliff, field time was reduced by ~80% compared to using a TLS (James & Robson, 2012). Above all, the elevations derived from images can have a comparable level of accuracy to the conventional surveys and survey errors have minimal impact on data analysis in comparison to the degree of beach variability.

However there are also several limitations associated with these methods. The images cannot be taken during the night or low visibility – just as any other visible-light remote sensing techniques. Also, because images are required from different angles and distances, there is still need for data to be taken manually.

This usually restricts data acquisition to times of favourable conditions (such as during calm weather conditions) and some important dynamics may be missed. Unlike video and in particular photogrammetry using a pair of video cameras, images cannot be taken at high temporal resolution (e.g. at intervals less than an hour or so, but depending on the project scale). Also, one might argue that the data presented here were selected due to advantageous site-specific features, such as clearly pronounced features and textures (e.g. gravel, berms and ridges), clear conditions, good viewing angles and relatively easy access. Future work will include more rigorous and quantitative evaluation of techniques described here, under a broader range of conditions.

The different approaches used here may appeal to different users. 123D Catch carries out the bulk of the data processing remotely, but the results are less easy to geo-reference. Using a local SfM-MVS reconstruction pipeline requires a computer for the intensive image processing, but provides more information that can be used to assess error magnitudes. There also remains significant scope to improve the current procedures for a broad range of environmental applications. For example, reducing the number of images processed can decrease reconstruction time, and strategies for more efficient data collection can be developed.

5. Conclusion

The examples presented here demonstrate 3D models of sufficient quality for valuable use in visualizing and quantifying coastal change. Importantly, SfM-MVS-based techniques are convenient for frequent acquisition of high-resolution 3D data at a fraction of the time and cost of alternative approaches. However, the SfM-MVS is not without limitations, and different software implementations have different advantages. The reconstruction precision is dependent on the locations and distances from which images are taken and the number and quality of images. Overall accuracy is also dependent on the availability of suitable sites for geo-referencing. Whilst 123D Catch carries out the computing intensive reconstruction on remote servers, the resulting models are more difficult to geo-reference than those from locally run SfM-MVS. Future work will include guidelines for data collection and processing for different coastal applications in order to understand and improve the accuracy of these techniques.

Acknowledgements

The authors would like to thank to the British Oceanographic Data Centre for supplying the tidal data at Heysham, the Channel Coastal Observatory for providing the wave data from the Morecambe buoy and Florine Dehay who took images of vegetation tussocks in Morecambe during her internship in the Lancaster Environment Centre in the summer 2011.

References

Bouma, T.J., van Duren, L.A., Temmerman, S., Claverie, T., Blanco-Garcia, A., Ysebaert, T. and Herman, P.M.J. 2007. Spatial flow and sedimentation patterns within patches of epibenthic structures: Combining field, flume and modelling experiments. *Continental Shelf Research*, 27: 1020-1045.

Castillo, C., Perez, R., James, M.R., Quinton, N.J., Taguas, E.V. and Gomez, J.A. 2012. Comparing the accuracy of several field methods for measuring gully erosion, *Soil Science Society of America Journal*, 76: 1319-1332, doi: 10.2136/sssaj2011.0390.

French, P.W. and Livesey, J.S. 2000. The impacts of fish-tail groynes on sediment deposition at Morecambe, North-West England. *Journal of Coastal Research*, 16(3): 724-734.

Furukawa, Y. and Ponce, J., 2010. Accurate, dense, and robust multiview stereopsis, *IEEE Trans. Pattern Anal. Mach. Intell.*, 32: 1362-1376.

Greenwood, R.O., and Orford, J.D. 2008. Temporal patterns and processes of retreat of drumlin coastal cliffs – Strangford Lough, Northern Ireland. *Geomorphology*, 94: 153 – 169.

Harley, M.D., Turner, I.L., Short, A.D. and Ranasinghe, R. 2011. Assessment and integration of conventional, RTK-GPS and image derived beach survey methods for daily to decadal coastal monitoring, *Coastal Engineering*, 58:

194-205.

Plant, N.G. and Holman, R.A., 1997. Intertidal beach profile estimation using video images. *Mar. Geol*.,140: 1-24.

James, M.R. and Robson, S., 2012. Straightforward reconstruction of 3D surfaces and topography with a camera: Accuracy and geosciences application, *J. Geophys. Res*., 117: F03017, doi: 10.1029/2011JF002289.

Moxon, A.J. 2011. Controls on cliff erosion at Sunderland Point, Lancashire, *MRes dissertation*, Lancaster Environment Centre, Lancaster University, U.K.

Rosser, N.J., Petley, D.N., Lim, M., Dunning, S.A. and Allison, R.J. 2005. Terrestrial laser scanning for monitoring the process of hard rock coastal cliff erosion, *Quart. J. Eng. Geology Hydrol*., 38: 363-375.

Snavely, N., Garg, R., Seitz, S.M. and Szeliski, R., 2008. Modeling the world from internet collection, *Int. J. Comput. Vis*., 80: 189-210.

Stockdon, H.F., Sallenger, A.H., List, J.H. and Holman, R.A., 2002. Estimation of shoreline position and change using airborne topographic lidar data. *J. Coastal Res*., 18(3): 502-513.

Sallenger, A.H., Krabill, W.B., Swift, R.N., Brock, J., List, J., Hansen, M., Holman, R.A., Manizade, S., Sontag, J., Meredith, A., Morgan, K., Yunkel, J.K., Frederick, E.B., Stockdon, H. 2003. Evaluation of airborne topographic lidar for quantifying beach changes. *Journal of Coastal Research*, 19(1): 125-133.

Young, A.P., Guza, R.T., Flick, R.E., O'Reilly, W.C. and Gutierrez, R. 2009. Rain, waves and short-term evolution of composite sea cliffs in Southern California. *Marine Geology*, 267: 1-7.

Weir, F.M., Hughes, M.G. and Baldock, T.E. 2006. Beach face and berm morphodynamics fronting a coastal lagoon. *Geomorphology*, 82: 331-346.